

Degradation of Phenol in Water Using a Novel Gas-Liquid Two-Phase Dielectric Barrier Discharge Plasma Reactor

Han Zhang · Yanan Liu  · Xi Cheng · Ai Zhang · Xiang Li · Jinxia Liu · Shijie Cai · Cheng Yang · Stéphanid Ognier · Pan Li

Received: 22 June 2018 / Accepted: 29 August 2018 / Published online: 11 September 2018
© Springer Nature Switzerland AG 2018

Abstract Phenol is toxic to human and persistent in the environment. Traditional treatment methods have the disadvantages of long treatment time, large amount of agents, and secondary pollution. In this study, a novel gas-liquid two-phase dielectric barrier discharge reactor was designed to remove phenol in aqueous solution. The effects of operating conditions (applied voltage,

discharge spacing, pH, and conductivity), different water matrix (deionized water, groundwater, surface water, tap water), and inorganic ions were investigated. Moreover, the reaction mechanisms and the possible degradation pathway were proposed. The removal efficiency of phenol achieved 95.5% under the optimal operating conditions (discharge voltage of 17.6 kV, discharge gap of 1 mm, air flow rate of 60 mL min⁻¹) coupling with H₂O₂ at 10 mM. The presence of different concentrations of inorganic ions (0.1, 1, 10, and 20 mM) could inhibit the phenol removal efficiencies. Specially, Cl⁻ had different effects on phenol removal efficiency. The inhibition of Cl⁻ on phenol removal was weakened when Cl⁻ concentration was greater than 1 mM, which allows the technology that has certain advantages in treating high-salt wastewater containing high chloride concentration. In addition, ·OH was verified as the main active species in phenol removal. The possible degradation pathway was proposed according to theoretical calculation and GC-MS measurement.

Electronic supplementary material The online version of this article (<https://doi.org/10.1007/s11270-018-3968-x>) contains supplementary material, which is available to authorized users.

H. Zhang · Y. Liu · X. Cheng · A. Zhang · X. Li · S. Cai · C. Yang
College of Environmental Science and Engineering, Donghua University, 2999 North Renmin Road, Shanghai 201620, People's Republic of China

Y. Liu (✉)
Shanghai Institute of Pollution Control and Ecological Security, Shanghai 200092, China
e-mail: liuyanana@dhu.edu.cn

J. Liu
Department of Civil Engineering, McGill University, Montreal PQ H3A 0C3, Canada

S. Ognier
Institut de Recherche de Chimie Paris (IRCP), Equipe 2PM (Procédés, Plasmas, Microsystèmes), UMR 8247, ChimieParisTech-CNRS, 11 Rue Pierre et Marie Curie, 75005 Paris, France

P. Li
School of Environmental Science and Engineering, State Key Laboratory of Control and Resource Reuse, Tongji University, 1239 Siping Road, Shanghai, People's Republic of China

Keywords Phenol · Gas-liquid two-phase dielectric barrier discharge plasma · Radicals · Degradation pathway

1 Introduction

Phenol and its derivatives are a large group of aromatic hydrocarbons existing in groundwater and surface water (Zhu et al. 2007). Their primary sources are the activities of industrial factories, such as refinery, petrochemical

processing, pulp and paper, plastic, paint, textile, pesticide, and chemical factories (Krugly et al. 2015). Phenols are listed as the priority pollutant due to its high toxicity and persistence in the environment (Narengerile et al. 2011). The discharge of phenol has been strictly regulated by the Integrated Wastewater Discharge Standard, and it is classified as the second type of pollutant with a maximum emission concentration of 0.5 mg/L. Therefore, its removal from wastewater is a practical and important problem.

Methods commonly used in phenol removal include extraction (Xu et al. 2006), adsorption (Lin and Juang 2009), membrane filtration (López-Muñoz et al. 2009), biological degradation (Vidya Shetty et al. 2007), electrochemical oxidation (Li et al. 2005), photocatalytic degradation (Busca et al. 2008; Wang et al. 2005), and ozonation (Chedeville et al. 2007). However, most of these treatment techniques have their own disadvantages. For example, physical adsorption has the disadvantages of blockage of adsorbent and poor regeneration. The biological degradation of phenol needs a long treatment time and is greatly influenced by environmental factors (pH value, temperature, oxygen, etc.). Some advanced oxidation processes require chemical agents, and most of these chemicals are harmful to the environment, or cause the secondary pollution. Therefore, the development of environmentally friendly and efficient methods to remove phenol from water receives great attention.

In the past few years, non-thermal plasma treatment has attracted more attention as a green and effective technology for the removal of hazardous organic contaminants because of its resulting processes simple, effective, and easy for further technological transfer and do not require other chemical agents. During the discharge plasma process, a large number of chemically active species are formed, such as O_3 , H_2O_2 , radicals ($\cdot OH$, $HO_2\cdot$, $H\cdot$, and $O\cdot$, etc.) and ions (O_2^- , O_2^+ , O_3^-). Simultaneously, physical effects can be induced in the pollutant removal process, such as strong electric field, ultraviolet light, shock waves, and high-temperature pyrolysis (Krugly et al. 2015; Wang et al. 2014, 2015a, b). As one of the non-thermal plasma technologies, dielectric barrier discharge (DBD) can also produce a variety of active species by the cooperative effects of ozone oxidation, high-energy electron radiation, and UV photolysis. Furthermore, compared to other plasma technologies, DBD is considered to be an effective discharge technology because of its easy to scale-up to large dimensions and the stable and micro-

discharge over the entire discharge area (Jiang et al. 2014; Wu et al. 2015; Xue et al. 2008). Hybrid gas-liquid discharge is an effective discharge mode for removing pollutants in aqueous solution. In this discharge mode, discharge happens at the interface between gas and liquid phases and then forms hybrid gas-liquid two phases fluid, which increases the contact areas of plasma and pollutant molecules.

In this study, the degradation of phenol with a self-designed DBD reactor was investigated. Several discharge parameters affecting the phenol degradation, such as applied voltage, discharge spacing, pH, and conductivity, were discussed in detail. Specifically, the effects of different water matrix and the presence of different ions (CO_3^{2-} , SO_4^{2-} , NO_3^- , and Cl^-) on phenol removal were also investigated. The main active species during the process were clarified. Moreover, the possible degradation pathway of phenol by DBD treatment was also studied.

2 Materials and Methods

2.1 Materials

All of the reagents, including phenol (CAS: 108-95-2), sodium chloride (NaCl), anhydrous sodium carbonate (Na_2CO_3), sodium sulfate (Na_2SO_4), sodium nitrate ($NaNO_3$), hydrogen peroxide (H_2O_2), and tertiary butyl alcohol (TBA) were of analytical grade and purchased from Sinopharm Chemical Reagent Co., Ltd. Phenol solution was prepared with deionized water to 1.06 mM (direct preparation when used). The initial pH of the solution was adjusted by adding hydrochloric acid (HCl) and sodium hydroxide (NaOH) solution, and the solution conductivities were adjusted by sodium chloride (NaCl). Other solutions used in the experiment were also prepared with deionized water.

2.2 Experimental Apparatus

A schematic diagram of the experimental apparatus is shown in Fig. 1. The experimental system mainly consisted of four parts: a high-voltage alternating current power source, a DBD reactor, a contact voltage regulator, and a gas delivery system.

The discharge was generated in a DBD reactor with cylindrical geometry. The reactor was made of two coaxial cylindrical quartz glass tubes, with the solution

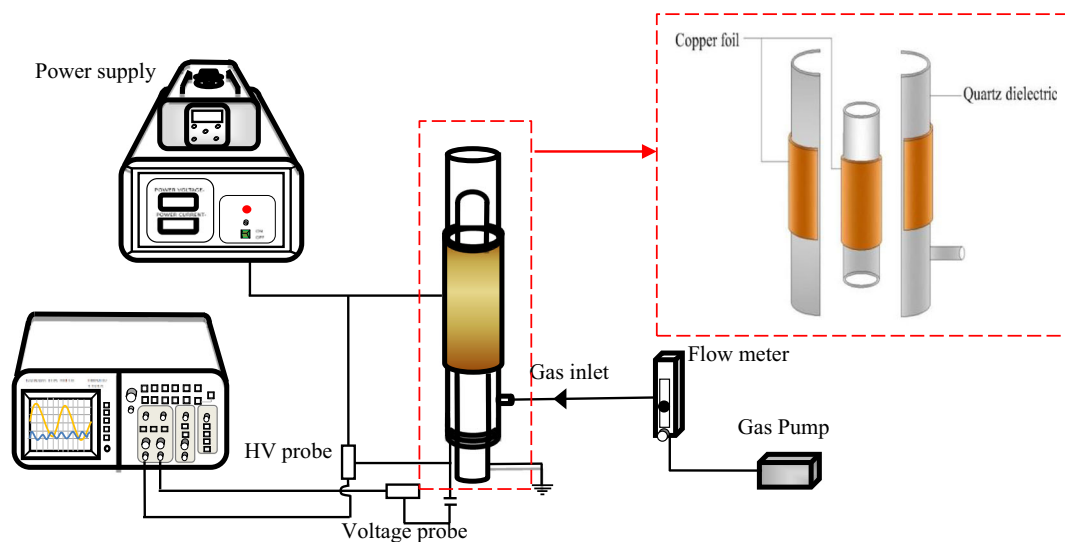


Fig. 1 Schematic diagram of the experimental system

placed in the gaps between the two tubes. The copper foil wrapped on the two tubes acted as high-voltage electrode and ground electrode. The DBD reactor we used was a single dielectric barrier reactor, and the copper foil was pasted on the outer side of the two cylinders. The inner diameters of the outer tubes were 17 mm, and the outside diameter of the inner tube was 15 mm. The air was pumped into the reactor by an air pump. A gas flow meter was used to control the air flow rate of the reaction, which was connected with the pump and reactor through a rubber tube. In each reaction, phenol with an initial concentration of 1.06 mM was placed into the reactor, gas flow rate was 60 mL min^{-1} , and samples were taken after treatment for 2, 6, 12, 20, and 30 min, respectively.

2.3 Methods and Analyses

The voltage and capacitance voltage were measured by a Tektronix TDS2012B digital oscilloscope with a Tektronix P6015A high voltage probe and a Tektronix TPP0101 voltage probe. A pH meter (PHS-3E, Shanghai Green Electronics Co., Ltd.) was used to measure the pH variation during the plasma treatment. A conductivity meter (3020M, JENCO Instrument Co., Ltd) was used to measure the conductivities of solution during the plasma treatment.

Phenol was determined with a UV-Vis spectrophotometry with 4-aminoatipyrine as an indicator. After adding potassium ferricyanide to the samples in alkaline medium, red-orange antipyrine dye was formed. The

absorbance measured at the wavelength of 510 nm, and the concentration of phenol could be calculated based on the standard curve (Fig. S1). Most of the experiments were performed in duplicate or triplicate, and average data are reported.

The identification of phenol and its by-products were determined using a gas chromatography–mass spectrometry (GC–MS, QP-2010Ultra) with a 20-m long fused-silica capillary column (DB-5, J&W Scientific, USA). The internal diameter and film thickness of the fused-silica capillary column were 0.25 and 0.25 μm , respectively. The temperature program began at $40 \text{ }^\circ\text{C}$ for 2 min and increased at a rate of $15 \text{ }^\circ\text{C min}^{-1}$ up to $280 \text{ }^\circ\text{C}$, with a holding time of 10 min. Helium (99.999% pure) served as the carrier gas at a constant flow rate of 1.0 mL min^{-1} . The samples were extracted by solid phase micro extraction.

3 Results and Discussion

3.1 Effects of Applied Voltage and Discharge Spacing

In order to optimize the efficiency of DBD reactor in phenol removal, different peak voltages and discharge spacing were investigated with results shown in Fig. 2.

As shown in Fig. 2a, the removal efficiency of phenol increased with the increase of peak voltage from 15.2 to 17.6 kV. 11.5% of phenol was removed after 30 min of DBD treatment with applied peak voltage of 15.2 kV, while 63.9% was removed with peak voltage of 17.6 kV

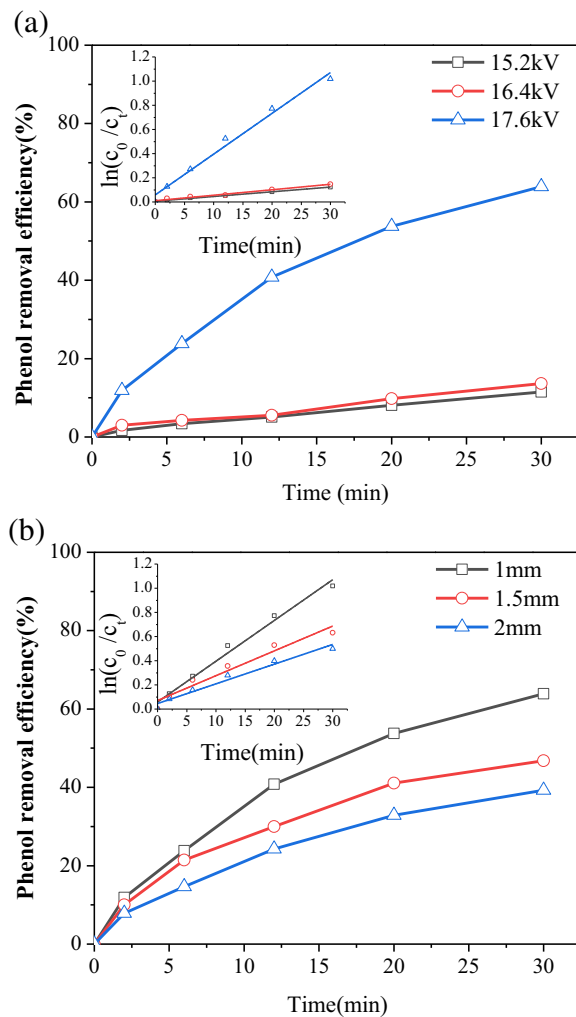


Fig. 2 Influences of input powers (a) (pH unadjusted, initial phenol concentration = 1.06 mM) and treatment distance (b) (pH unadjusted, initial phenol concentration = 1.06 mM) on the effect of phenol removal efficiency

under the same experimental conditions. The degradation curve follows a first-order kinetic model (the inset figure in Fig. 2a). As presented, with the peak voltage increased from 15.2 to 17.6 kV, the reaction rate constant increased from 0.0037 to 0.0321. The results showed that higher removal rate of phenol could be obtained at higher peak voltage, and all of $R^2 > 0.9$ also indicated that the results were credible. The increase of phenol removal efficiency can be explained by the positive correlation between input energy and number of active species produced during discharge (Jiang et al. 2014; Tang et al. 2016; Wang et al. 2015a). When increasing the discharge voltage, the input energy and electric field intensity will be increased, resulting in

more energetic electrons producing and accelerating the formation of active species. Meanwhile, the physical effects during the discharge process would also become stronger at higher applied voltages (Tang et al. 2013).

Figure 2b shows the removal of phenol at various discharge spacing. The discharge spacing of 1, 1.5, and 2 mm were tested. As can be seen, phenol removal increased from 39.3% with a discharge gap distance of 2 mm to 63.9% with that of 1 mm. On the one hand, the effect of eddies and water circulation caused by convection currents will change in different discharge spacing; on the other hand, the charged particles can easily reach the surface of the barriers when the discharge gap is smaller, so that the electric field intensity will increase as the surface charges increases (El-Tayeb et al. 2016; Liu et al. 2017), which leading to an enhancement of the number of active species in the discharge zone. Therefore, the removal efficiency of phenol was increased by decreasing discharge spacing.

3.2 Effects of Initial pH and Conductivity

Solution condition is one of the most important factors that influence the removal efficiency of pollutants during AOPs. Since pH and conductivity are important solution conditions for organic compounds degradation in DBD plasma system (Wang and Chen 2011), the effects of different initial pH and conductivity on phenol removal were studied in this section.

The effect of initial solution pH on phenol removal efficiency was shown in Fig. 3a. The initial pH of phenol solution was 6.8 without pH adjustment. In order to understand the effect of pH on phenol removal, the initial pH of the solution was adjusted to 3.1, 8.0, and 11.0, respectively. When solution pH increased from 3.1 to 6.8, phenol removal efficiency improved from 32.9 to 63.9%. However, the removal efficiency decreased gradually when solution pH continues rising to 11.0. Compared with the pH value of 6.8, the removal efficiency decreased to 56.0 and 22.9% for the solution pH of 8.0 and 11.0, respectively. The highest removal efficiency was achieved at pH 6.8. This result is similar to the result of Duan et al. (2013).

The pH value is an important factor for hydroxyl radical production and ozone decomposition in solution. Under acidic conditions, the generation of $\cdot\text{H}$ consumes a large number of electrons, reducing the formation of activated species such as $\cdot\text{OH}$ and O_3 (Eq. (1)) (Wu et al. 2015; Singh et al. 2016). In addition, there are two

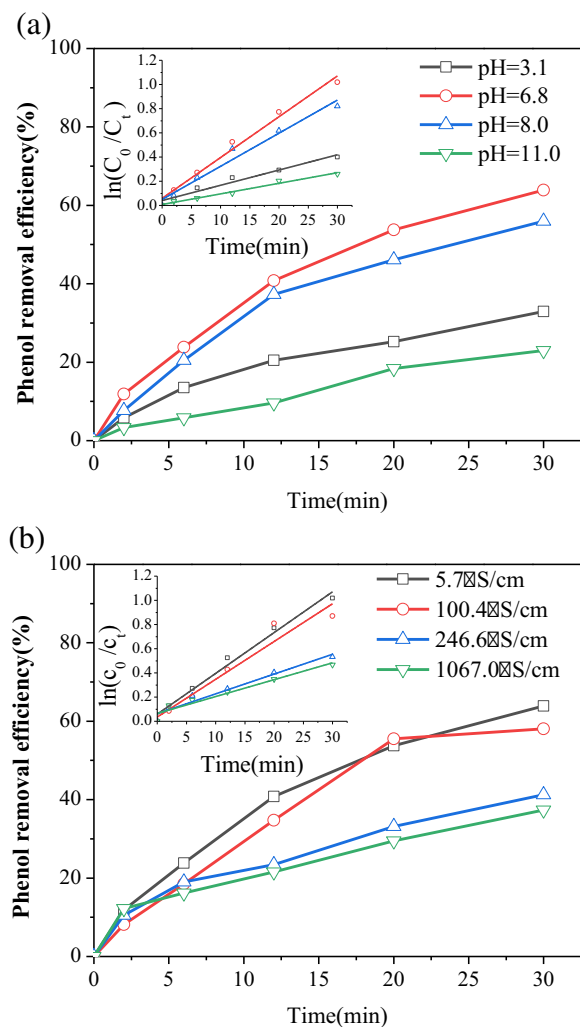
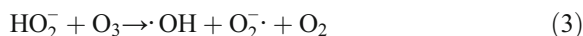


Fig. 3 Influences of initial pH (a) (initial solution pH=3.1, 6.8, 8.0, and 11.0) and conductivity (b) (initial conductivity = 5.7, 100.4, 246.6 and 1067.0 $\mu\text{S cm}^{-1}$) on the effect of phenol removal efficiency

different reaction routes to degrade pollutants through ozone oxidation under different pH values: oxidized directly by ozone and oxidized by active species with high-reactivity, which are formed through ozone decomposition (Duan et al. 2013; Wang et al. 2007). Ozone is relatively stable under acidic medium, but it can be decomposed under alkaline conditions to accelerate the formation of $\cdot\text{OH}$ (Khuntia et al. 2015; Xue et al. 2008). Therefore, the direct ozonation pathway would dominate under acidic condition. Meanwhile, the oxidation potential of ozone under acid conditions (1.25 V) is lower than that of $\cdot\text{OH}$ (2.8 V) (Xue et al. 2008; Li et al. 2015; Khuntia et al. 2016). Hence, the removal efficiency of

phenol in acidic conditions is lower. In alkaline conditions, ozone and hydrogen peroxide are easily decomposed to form $\cdot\text{OH}$, thus improving the removal efficiency of phenol (Eqs. (2)–(3)) (Vanraes et al. 2017; Duan et al. 2013). However, it is easy to form CO_3^{2-} or HCO_3^- in solution when $\cdot\text{OH}$ radicals decompose phenol into inorganic carbon (Eqs. (4)–(5)) (Wu et al. 2015). Furthermore, the excess hydrogen peroxide can also react with the $\cdot\text{OH}$ to form $\cdot\text{HO}_2$, which is also a $\cdot\text{OH}$ scavenger (Bobkova et al. 2016; Gai 2007).

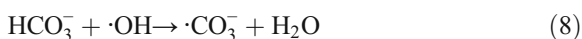


Initial conductivity is another important factor that affects the removal efficiency of phenol with the DBD system. To some extent, conductivity indicates the concentration of electrolytes in aqueous solution (Chen et al. 2004). The initial conductivity of phenol solution was $5.7 \mu\text{S cm}^{-1}$ without conductivity adjustment. Other solution conductivities in the experiment were adjusted to 100.4, 246.6, and $1067.0 \mu\text{S cm}^{-1}$, respectively. Figure 3b shows the change of removal efficiency of phenol under different conductivities. As the initial conductivity of solution increases, the removal efficiency of phenol decreases gradually. The reasons for this result can be analyzed from two aspects. On the one hand, the length of plasma channel determines the plasma-water contact area, which has an important role in the generation of reactive species. At the same time, the length of the plasma channel is negatively correlated with the conductivity, and the high conductivity shortened plasma channel lengths, thus affecting the removal of phenol (Liu et al. 2018). On the other hand, NaCl, which is used to regulate the conductivity, is known as a $\cdot\text{OH}$ scavenger, which can rapidly react with hydroxyl radical to produce non-active species, thus reducing the removal efficiency of phenol.

3.3 Effects of the Water Matrix and Inorganic Ions

Water quality is one of the most important factors influencing the formation of active species during discharge. In order to study the effects of water quality on phenol degradation by DBD, four different actual water matrix were tested. As can be seen from Fig. 4a, the removal efficiency of phenol in actual water matrix decreased obviously compared with deionized water. After a reaction time of 30 min, the phenol removal efficiencies were 63.9% in deionized water, 48.7% in groundwater, 29.4% in surface water, and 18.6% in tap water. The above phenomena may be explained by the amounts of ions in actual water body, which have a great influence on phenol removal (water quality indexes of different water matrix are shown in Table S2).

Therefore, in order to investigate the influence of ions on phenol degradation with DBD, four different inorganic salts (Na_2CO_3 , NaCl , NaNO_3 , and Na_2SO_4) were tested. As can be seen from Fig. 4b, when different concentrations of Na_2CO_3 (0.1, 1, 10, and 20 mM) were added into the solution, the removal efficiencies of phenol dropped dramatically from 63.9 to 15%. $\text{CO}_3^{2-}/\text{HCO}_3^-$ are considered to be effective $\cdot\text{OH}$ scavengers (López Peñalver et al. 2013). In this case, the active species used to degrade phenol are reduced, resulting in a decrease on phenol removal efficiency (Vanraes et al. 2017).



Although secondary radical $\text{CO}_3^{\cdot-}$ ($E^0 = 1.59$ V) could be formed, its oxidation potential is much lower than that of $\cdot\text{OH}$ ($E^0 = 2.8$ V) (Santiago et al. 2014; Zhang et al. 2017). In addition, the reaction rate constant of $\text{CO}_3^{\cdot-}$ ($1.6 \times 10^7 \text{ M}^{-1} \text{ s}^{-1}$) with phenol is much lower than that of $\cdot\text{OH}$ ($1.4 \times 10^{10} \text{ M}^{-1} \text{ s}^{-1}$), resulting in a negative effect on phenol removal (Marotta et al. 2012).

The effect of SO_4^{2-} on phenol removal was similar to that of CO_3^{2-} . The phenol removal efficiency after 30-min treatment decreased from 63.9 to 55.2, 29.8, 27.3, and 19.8% with SO_4^{2-} concentration of 0, 0.1, 1, 10, and 20 mM, respectively. SO_4^{2-} is a scavenger of $\cdot\text{OH}$ as shown in Eqs. (9)–(11). The $\cdot\text{SO}_4^-$ produced by Eq. (9) could also react with electrons to consume electrons

generated by plasma (Eq. (12)) (Santiago et al. 2014). Moreover, although $\cdot\text{SO}_4^-$ ($E^0 = 2.6$ V) almost have the similar oxidation capacity as $\cdot\text{OH}$ ($E^0 = 2.8$ V), the reactivity of $\cdot\text{OH}$ is less selective than that of $\cdot\text{SO}_4^-$ (Dojcinovic et al. 2012)

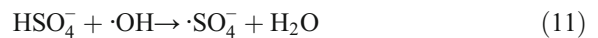
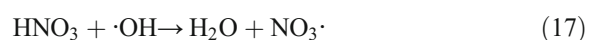
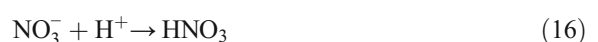


Figure 4d shows the influence of NO_3^- on phenol removal by DBD reactor. The addition of NO_3^- exhibited obvious inhibiting effects on the removal of phenol. About 63.9% of phenol was degraded after 30-min discharge without NaNO_3 addition, while the removal rate was reduced to 18.9% with 20-mM NaNO_3 addition. This might be attributed to the reactivity of NO_3^- with e_{aq}^- . NO_3^- can react rapidly with e_{aq}^- , while the formation of active species might be dependent on e_{aq}^- to a certain extent (Wang et al. 2015a) (Eqs. (13)–(15)). Moreover, NO_3^- has strong absorption in the UV region, which will prevent the light through the solution and is used as the inert filter (Sorensen and Frimmel 1997). The inhibition effect of inert filter is stronger than $\cdot\text{OH}$ produced by NO_3^- , which leads to the inhibition of phenol removal; at the same time, NO_3^- could react with $\cdot\text{OH}$ with a reaction rate constant of $1.4 \times 10^8 \text{ M}^{-1} \text{ s}^{-1}$ (Eq. (16)).



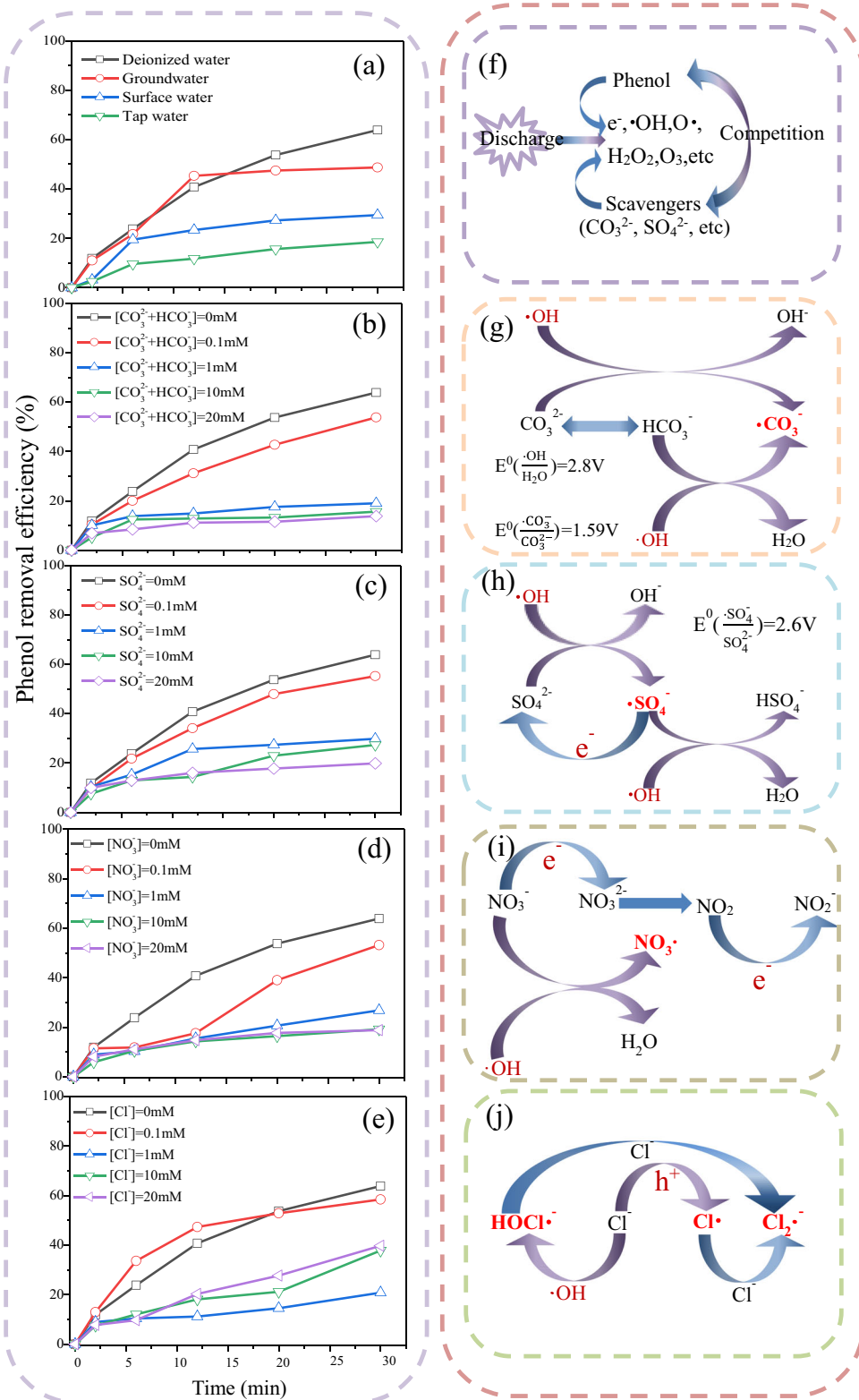
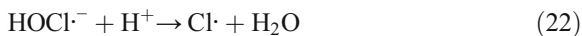


Fig. 4 Influences of different water matrix and inorganic ions on the effect of phenol removal efficiency (a–e), mechanism diagrams of adding different inorganic ions (f–j)

Cl^- extensively existed in natural water, because it is an essential disinfectant in the chlorination process of drinking water (Zhang et al. 2017). Figure 4e shows the influence of Cl^- at different concentrations on phenol removal and its effect on phenol is different from that of the other three ions. When the concentration of chloride ions increased from 0 to 1 mM, the removal efficiency of phenol decreased from 63.9 to 20.9%. However, the inhibition of Cl^- was weakened with the increase of Cl^- amount from 1 to 20 mM. It can be explained by the following reactions:



As a scavenger of $\cdot\text{OH}$ and h^+ , Cl^- could reduce the phenol removal at low concentration (Eqs. (18)–(19)) (Santiago et al. 2014). Whereas, Liao et al. (2001) found that $\cdot\text{OH}$ did not decrease with the increase of the concentration of Cl^- when Cl^- concentration increased to a certain extent due to the release of $\cdot\text{OH}$ from HOCl^- . Meanwhile, the hydrophobicity of phenol increased with the increase of Cl^- concentration, causing the movement of phenol molecules from the solution to the gas-liquid interface, thus increasing the interface phenol concentration (Guo et al. 2008; Mahamuni and Pandit 2006). This increased the possibility of $\cdot\text{OH}$ reacting with phenol, thus increasing the removal efficiency of phenol. At the same time, $\cdot\text{Cl}$ and $\cdot\text{Cl}_2$ also have certain oxidative ability, which can further react with phenol.

3.4 Probable Degradation Mechanism of Phenol

As is shown in Fig. 5a, the percentage removal of phenol increased significantly by increasing the concentration of H_2O_2 from 0 to 10 mM. After 30 min of discharge, the removal efficiency of phenol increased

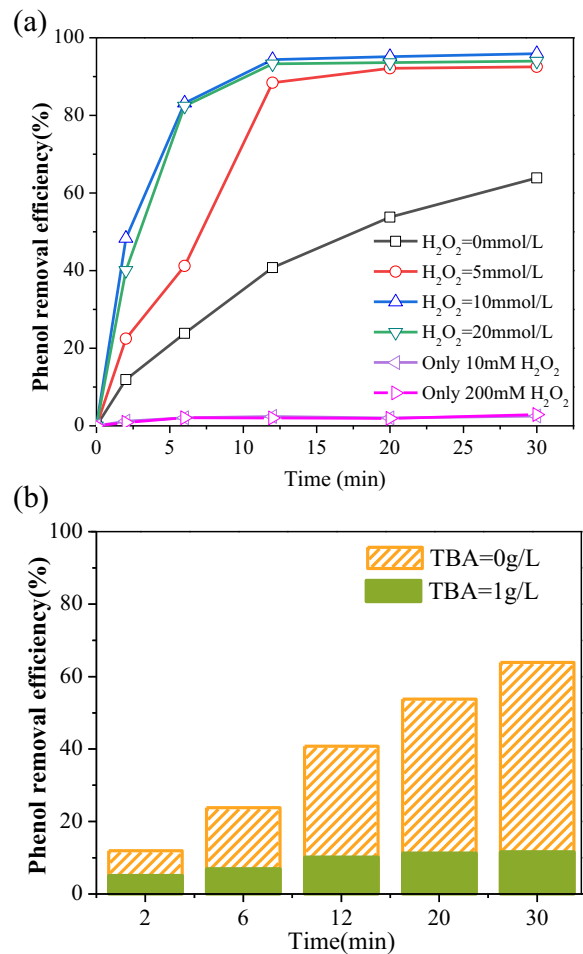
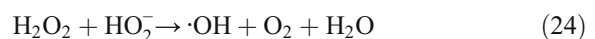
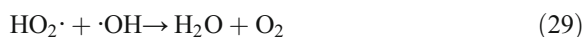
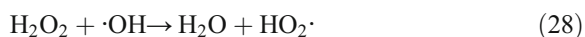
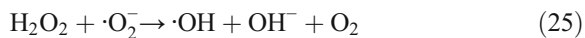


Fig. 5 Influences of H_2O_2 (a) and TBA (b) on the effect of phenol removal efficiency

to 95.5% with H_2O_2 concentration of 10 mM. However, when the concentration of H_2O_2 increased to 20 mM, the removal efficiency showed no difference compared with that of 10 mM.

H_2O_2 is known to be able to be decomposed by the active species and ultraviolet radiation generated by DBD, forming hydroxyl radicals and oxygen (Eqs. (23)–(27)) (Sun et al. 2000; Wu et al. 2015; Gai 2007; Mercado-Cabrera et al. 2017; Feng et al. 2008). However, excessive hydrogen peroxide would consume hydroxyl radicals, producing less effective active species, thus inhibiting the degradation of phenol (Eqs. (28)–(29)).





In view of the results of Fig. 5a and the high reaction rate constant ($10^9 \text{ M}^{-1}\text{s}^{-1}$) (An et al. 2011) between phenol and $\cdot\text{OH}$, we investigated the role of $\cdot\text{OH}$ in phenol degradation in this study. TBA is a stable $\cdot\text{OH}$ scavenger and it is difficult to be oxidized or dehydrogenated. Its bimolecular reaction rate constant with $\cdot\text{OH}$ is $4.56 \times 10^{10} \text{ M}^{-1} \text{ min}^{-1}$. When adding TBA to phenol solution, it can react with $\cdot\text{OH}$ to form inert intermediates and terminates the chain decomposition reaction of ozone, thus hindering the reaction of $\cdot\text{OH}$ with phenol (Arslan-Alaton and Caglayan 2005; Li et al. 2016). As shown in Fig. 5b, the removal efficiency decreased obviously with the presence of TBA. This result

clearly certified that $\cdot\text{OH}$ is the main active species in phenol degradation with DBD.

The degradation intermediates of phenol by the DBD plasma were analyzed with GC-MS. GC-MS spectrums of the solution after 12 min of DBD and 30 min of plasma treatment are shown in Figs. S2–S3. As shown in Table S1, the main products produced after 12 min of DBD treatment were oxalic acid and malonic acid, while after 30 min of treatment, only one by-product (malonic acid) was detected.

As the frontier orbital theory (FOT) states, in electrophilic reactions, the most vulnerable position is the atom of the highest charge density in the highest occupied molecular orbital (HOMO) of the aromatic molecules. The spatial configuration and electron cloud density distribution of phenol molecules could be obtained by molecular orbital calculations, which could help in the prediction of the degradation behavior of phenol. Therefore, Gaussian software was employed with the density function theory method.

Figure 6 and Table 1 show the total charge density, the lengths, angles, and atomic charges of the main structure in phenol molecule, respectively. Due to the stronger electron cloud and the relatively large rate constants of the para-position and ortho-position of phenol, $\cdot\text{OH}$ attacked them first and generated hydroquinone and catechol. Moreover, they could be further oxidized and formed 1,2-benzoquinone and benzoquinone due to the different electronegativity

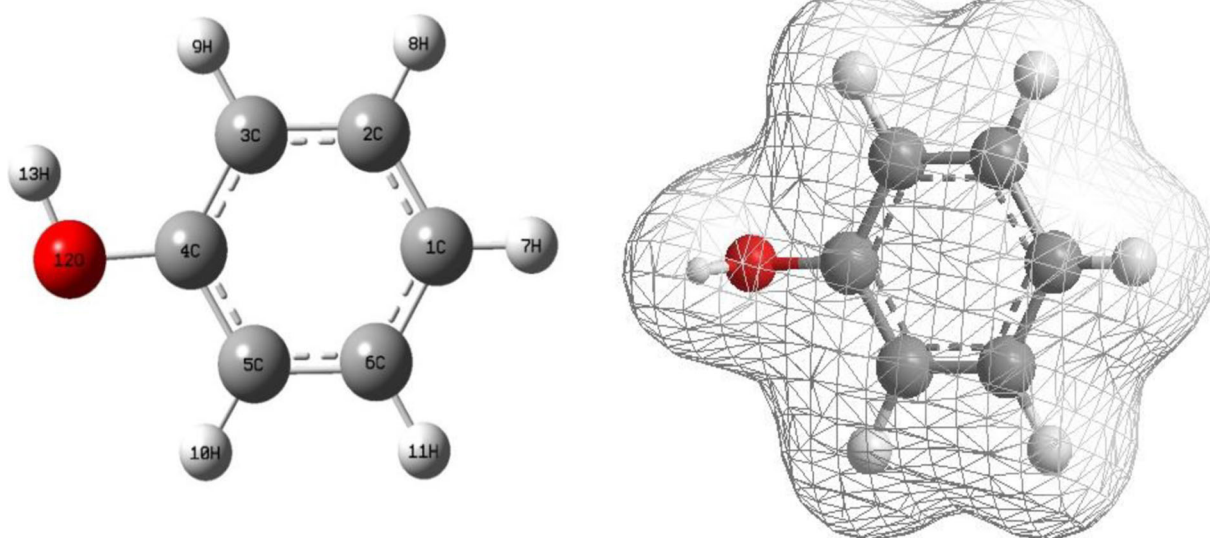
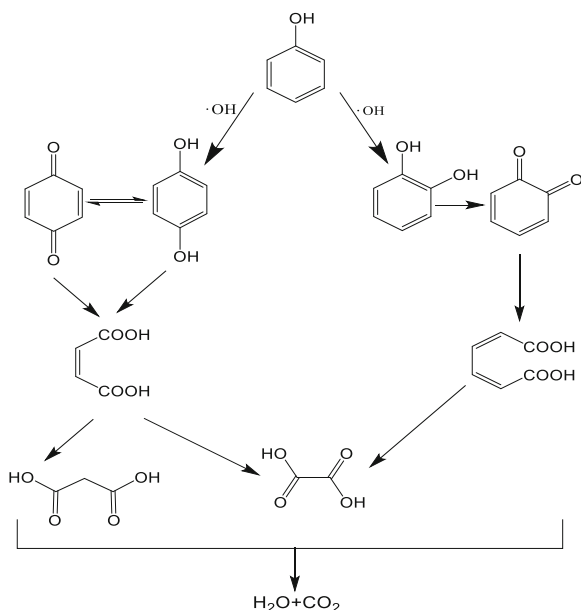


Fig. 6 Structure and total charge density of phenol

Table 1 Main bond lengths, bond angles and atomic charges of Phenol

Bond atoms	Length	Angle atoms	Angle	Atom	Atomic charges
C(1)—C(2)	1.395	C(3)—C(2)—C(1)	120.404	C(1)	-0.195
C(2)—C(3)	1.396	C(4)—C(3)—C(2)	120.172	C(2)	-0.185
C(3)—C(4)	1.398	C(5)—C(4)—C(3)	119.502	C(3)	-0.219
C(4)—C(5)	1.400	C(6)—C(5)—C(4)	120.099	C(4)	0.285
C(5)—C(6)	1.392	C(2)—C(1)—H(7)	120.341	C(5)	-0.186
C(1)—C(6)	1.395	C(1)—C(2)—H(8)	120.135	C(6)	-0.187
C(1)—H(7)	1.083	C(2)—C(3)—H(9)	119.854	H(7)	0.183
C(2)—H(8)	1.084	C(4)—C(5)—H(10)	118.241	H(8)	0.188
C(3)—H(9)	1.086	C(5)—C(6)—H(11)	119.421	H(9)	0.174
C(5)—H(10)	1.082	C(3)—C(4)—O(12)	123.446	H(10)	0.201
C(6)—H(11)	1.084	C(4)—O(12)—H(13)	109.904	H(11)	0.188
C(4)—O(12)	1.388			O(12)	-0.600
O(12)—H(13)	0.992			H(13)	0.353

of O and H atom. Then, the benzene ring was opened due to the different bond length and bond energy between C—C bonds and generated small molecules (Dai et al. 2008). Eventually, these small molecules were further mineralized to CO₂ and H₂O. The oxidation pathway for phenol was assumed on the basis of the GC-MS results and structure information. The possible reaction pathways are shown in Fig. 7.

**Fig. 7** Proposed reaction pathways for phenol degradation

4 Conclusions

In this paper, the degradation efficiency and mechanism of phenol solution were investigated using a self-designed gas-liquid two-phase DBD plasma reactor. The influence of discharge voltage, treatment time, discharge spacing, initial pH, electric conductivity, different water matrix, addition of hydrogen peroxide, and inorganic anions on phenol removal was studied. Under the optimal operating conditions, phenol removal (as high as 95.5% in 30 min combined with 10-mM H₂O₂) reached a stable state. Hydroxyl radical was verified to be the dominant active species. While different kinds of natural water matrix had negative effects on phenol removal, the presence of different concentrations of inorganic ions could inhibit the removal efficiencies. Different from other ions, Cl⁻ has two effects on phenol removal: a maximum inhibition at 1 mM, which weakens as concentration rises beyond 1 mM. The possible oxidation pathways of phenol were proposed based on the by-products analysis with GC-MS and DFT calculations.

Funding Information This work was completed by the financial support of the National Natural Science Foundation of China (No. 51578122, 51708096), the innovative training program for College Students and the China Postdoctoral Science Foundation (No. 2017M611423). All the financial supports are gratefully acknowledged.

References

- An, G., Sun, Y., Zhu, T., & Yan, X. (2011). Degradation of phenol in mists by a non-thermal plasma reactor. *Chemosphere*, 84(9), 1296–1300. <https://doi.org/10.1016/j.chemosphere.2011.05.007>.
- Arslan-Alaton, I., & Caglayan, A. E. (2005). Ozonation of procaine penicillin G formulation effluent. Part I: process optimization and kinetics. *Chemosphere*, 59(1), 31–39. <https://doi.org/10.1016/j.chemosphere.2004.10.014>.
- Bobkova, E. S., Krasnov, D. S., Sungurova, A. V., Rybkin, V. V., & Choi, H.-S. (2016). Phenol decomposition in water cathode of DC atmospheric pressure discharge in air. *Korean Journal of Chemical Engineering*, 33(5), 1620–1628. <https://doi.org/10.1007/s11814-015-0292-7>.
- Busca, G., Berardinelli, S., Resini, C., & Arrighi, L. (2008). Technologies for the removal of phenol from fluid streams: a short review of recent developments. *Journal of Hazardous Materials*, 160(2–3), 265–288. <https://doi.org/10.1016/j.jhazmat.2008.03.045>.
- Chedeville, O., Debacq, M., Ferrante Almanza, M., & Porte, C. (2007). Use of an ejector for phenol containing water treatment by ozonation. *Separation and Purification Technology*, 57(2), 201–208. <https://doi.org/10.1016/j.seppur.2007.04.004>.
- Chen, Y.-S., Zhang, X.-S., Dai, Y.-C., & Yuan, W.-K. (2004). Pulsed high-voltage discharge plasma for degradation of phenol in aqueous solution. *Separation and Purification Technology*, 34(1–3), 5–12. [https://doi.org/10.1016/S1383-5866\(03\)00169-2](https://doi.org/10.1016/S1383-5866(03)00169-2).
- Dai, Q., Lei, L., & Zhang, X. (2008). Enhanced degradation of organic wastewater containing p-nitrophenol by a novel wet electrocatalytic oxidation process: parameter optimization and degradation mechanism. *Separation and Purification Technology*, 61(2), 123–129. <https://doi.org/10.1016/j.seppur.2007.10.006>.
- Dojcinovic, B., Roglic, G., Obradovic, B., Kuraica, M., Tosti, T., Markovic, M., et al. (2012). Decolorization of reactive black 5 using dielectric barrier discharge in the presence of inorganic salts. *Journal of the Serbian Chemical Society*, 77(4), 535–548. <https://doi.org/10.2298/jsc110629179d>.
- Duan, L., Shang, K., Lu, N., Li, J., & Wu, Y. (2013). Study on the factors influencing phenol degradation in water by dielectric barrier discharge (DBD). *Journal of Physics: Conference Series*, 418, 012129. <https://doi.org/10.1088/1742-6596/418/1/012129>.
- El-Tayeb, A., El-Shazly, A. H., Elkady, M. F., & Abdel-Rahman, A. (2016). Simulation and experimental study for degradation of organic dyes using dual pin-to-plate corona discharge plasma reactors for industrial wastewater treatment. *Contributions to Plasma Physics*, 56(9), 855–869. <https://doi.org/10.1002/ctpp.201500080>.
- Feng, J., Zheng, Z., Sun, Y., Luan, J., Wang, Z., Wang, L., et al. (2008). Degradation of diuron in aqueous solution by dielectric barrier discharge. *Journal of Hazardous Materials*, 154(1–3), 1081–1089. <https://doi.org/10.1016/j.jhazmat.2007.11.013>.
- Gai, K. (2007). Plasma-induced degradation of diphenylamine in aqueous solution. *Journal of Hazardous Materials*, 146(1–2), 249–254. <https://doi.org/10.1016/j.jhazmat.2006.12.014>.
- Guo, Z., Feng, R., Li, J., Zheng, Z., & Zheng, Y. (2008). Degradation of 2,4-dinitrophenol by combining sonolysis and different additives. *Journal of Hazardous Materials*, 158(1), 164–169. <https://doi.org/10.1016/j.jhazmat.2008.01.056>.
- Jiang, B., Zheng, J., Qiu, S., Wu, M., Zhang, Q., Yan, Z., et al. (2014). Review on electrical discharge plasma technology for wastewater remediation. *Chemical Engineering Journal*, 236, 348–368. <https://doi.org/10.1016/j.cej.2013.09.090>.
- Khuntia, S., Majumder, S. K., & Ghosh, P. (2015). Quantitative prediction of generation of hydroxyl radicals from ozone microbubbles. *Chemical Engineering Research and Design*, 98, 231–239. <https://doi.org/10.1016/j.cherd.2015.04.003>.
- Khuntia, S., Majumder, S. K., & Ghosh, P. (2016). Catalytic ozonation of dye in a microbubble system: hydroxyl radical contribution and effect of salt. *Journal of Environmental Chemical Engineering*, 4(2), 2250–2258. <https://doi.org/10.1016/j.jece.2016.04.005>.
- Krugly, E., Martuzevicius, D., Tichonovas, M., Jankunaite, D., Rumskaitė, I., Sedlina, J., et al. (2015). Decomposition of 2-naphthol in water using a non-thermal plasma reactor. *Chemical Engineering Journal*, 260, 188–198. <https://doi.org/10.1016/j.cej.2014.08.098>.
- López-Muñoz, M. J., Sotto, A., Arsuaga, J. M., & Van der Bruggen, B. (2009). Influence of membrane, solute and solution properties on the retention of phenolic compounds in aqueous solution by nanofiltration membranes. *Separation and Purification Technology*, 66(1), 194–201. <https://doi.org/10.1016/j.seppur.2008.11.001>.
- López Peñalver, J. J., Gómez Pacheco, C. V., Sánchez Polo, M., & Rivera Utrilla, J. (2013). Degradation of tetracyclines in different water matrices by advanced oxidation/reduction processes based on gamma radiation. *Journal of Chemical Technology & Biotechnology*, 88(6), 1096–1108. <https://doi.org/10.1002/jctb.3946>.
- Li, S., Ma, X., Liu, L., & Cao, X. (2015). Degradation of 2,4-dichlorophenol in wastewater by low temperature plasma coupled with TiO₂ photocatalysis. *RSC Advances*, 5(3), 1902–1909. <https://doi.org/10.1039/c4ra10797g>.
- Li, X., Li, J., Bai, J., Dong, Y., Li, L., & Zhou, B. (2016). The inhibition effect of tert-butyl alcohol on the TiO₂ nanoassays photoelectrocatalytic degradation of different organics and its mechanism. *Nano-Micro Letters*, 8(3), 221–231. <https://doi.org/10.1007/s40820-015-0080-2>.
- Li, X. Y., Cui, Y. H., Feng, Y. J., Xie, Z. M., & Gu, J. D. (2005). Reaction pathways and mechanisms of the electrochemical degradation of phenol on different electrodes. *Water Research*, 39(10), 1972–1981. <https://doi.org/10.1016/j.watres.2005.02.021>.
- Liao, C. H., Kang, S. F., & Wu, F. A. (2001). Hydroxyl radical scavenging role of chloride and bicarbonate ions in the H₂O₂/UV process. *Chemosphere*, 44(5), 1193–1200.
- Lin, S. H., & Juang, R. S. (2009). Adsorption of phenol and its derivatives from water using synthetic resins and low-cost natural adsorbents: a review. *Journal of Environmental Management*, 90(3), 1336–1349. <https://doi.org/10.1016/j.jenvman.2008.09.003>.
- Liu, W., Ma, C., Cui, W., Yang, X., Wang, T., & Chen, X. (2017). Study of atmospheric-pressure glow discharge plasma jets based on analysis of electric field. *Applied Physics Letters*, 110(2), 024102. <https://doi.org/10.1063/1.4973815>.

- Liu, Y., Zhang, H., Sun, J., Liu, J., Shen, X., Zhan, J., et al. (2018). Degradation of aniline in aqueous solution using non-thermal plasma generated in microbubbles. *Chemical Engineering Journal*, *345*, 679–687. <https://doi.org/10.1016/j.cej.2018.01.057>.
- Mahamuni, N. N., & Pandit, A. B. (2006). Effect of additives on ultrasonic degradation of phenol. *Ultrasonics Sonochemistry*, *13*(2), 165–174. <https://doi.org/10.1016/j.ultsonch.2005.01.004>.
- Marotta, E., Ceriani, E., Schiorlin, M., Ceretta, C., & Paradisi, C. (2012). Comparison of the rates of phenol advanced oxidation in deionized and tap water within a dielectric barrier discharge reactor. *Water Research*, *46*(19), 6239–6246. <https://doi.org/10.1016/j.watres.2012.08.022>.
- Mercado-Cabrera, A., PeÑA-Eguiluz, R., LÓPez-Callejas, R., Jaramillo-Sierra, B., Valencia-Alvarado, R., RodrÍGuez-MÉNdez, B., et al. (2017). Novel electrode structure in a DBD reactor applied to the degradation of phenol in aqueous solution. *Plasma Science and Technology*, *19*(7), 075501. <https://doi.org/10.1088/2058-6272/aa6715>.
- Narengerile, Yuan, M.-H., & Watanabe, T. (2011). Decomposition mechanism of phenol in water plasmas by DC discharge at atmospheric pressure. *Chemical Engineering Journal*, *168*(3), 985–993. <https://doi.org/10.1016/j.cej.2011.01.072>.
- Santiago, D. E., Araña, J., González-Díaz, O., Alemán-Dominguez, M. E., Acosta-Dacal, A. C., Fernández-Rodríguez, C., et al. (2014). Effect of inorganic ions on the photocatalytic treatment of agro-industrial wastewaters containing imazalil. *Applied Catalysis B: Environmental*, *156–157*, 284–292. <https://doi.org/10.1016/j.apcatb.2014.03.022>.
- Singh, R. K., Babu, V., Philip, L., & Ramanujam, S. (2016). Disinfection of water using pulsed power technique: effect of system parameters and kinetic study. *Chemical Engineering Journal*, *284*, 1184–1195. <https://doi.org/10.1016/j.cej.2015.09.019>.
- Sorensen, M., & Frimmel, F. H. (1997). Photochemical degradation of hydrophilic xenobiotics in the UV/H₂O₂ process: influence of nitrate on the degradation rate of EDTA, 2-amino-1-naphthalenesulfonate, diphenyl-4-sulfonate and 4,4'-diaminostilbene-2,2'-disulfonate. *Water Research*, *31*(11), 2885–2891. [https://doi.org/10.1016/s0043-1354\(97\)00143-7](https://doi.org/10.1016/s0043-1354(97)00143-7).
- Sun, B., Sato, M., & Clements, J. (2000). Oxidative processes occurring when pulsed high voltage discharges degrade phenol in aqueous solution. *Environmental Science & Technology*, *34*(3), 509–513.
- Tang, S., Lu, N., Li, J., Shang, K., & Wu, Y. (2013). Improved phenol decomposition and simultaneous regeneration of granular activated carbon by the addition of a titanium dioxide catalyst under a dielectric barrier discharge plasma. *Carbon*, *53*, 380–390. <https://doi.org/10.1016/j.carbon.2012.11.028>.
- Tang, S., Yuan, D., & He, J. (2016). Adsorbability enhancement of macroporous resin by dielectric barrier discharge plasma treatment to phenol in water. *Journal of Chemistry*, *2016*, 1–8. <https://doi.org/10.1155/2016/6701828>.
- Vanraes, P., Ghodbane, H., Davister, D., Wardenier, N., Nikiforov, A., Verheust, Y. P., et al. (2017). Removal of several pesticides in a falling water film DBD reactor with activated carbon textile: energy efficiency. *Water Research*, *116*, 1–12. <https://doi.org/10.1016/j.watres.2017.03.004>.
- Vidya Shetty, K., Ramanjaneyulu, R., & Srinikethan, G. (2007). Biological phenol removal using immobilized cells in a pulsed plate bioreactor: effect of dilution rate and influent phenol concentration. *Journal of Hazardous Materials*, *149*(2), 452–459. <https://doi.org/10.1016/j.jhazmat.2007.04.024>.
- Wang, H. J., & Chen, X. Y. (2011). Kinetic analysis and energy efficiency of phenol degradation in a plasma-photocatalysis system. *Journal of Hazardous Materials*, *186*(2–3), 1888–1892. <https://doi.org/10.1016/j.jhazmat.2010.12.088>.
- Wang, W., Serp, P., Kalck, P., & Faria, J. L. (2005). Photocatalytic degradation of phenol on MWNT and titania composite catalysts prepared by a modified sol-gel method. *Applied Catalysis B: Environmental*, *56*(4), 305–312. <https://doi.org/10.1016/j.apcatb.2004.09.018>.
- Wang, H., Li, J., Quan, X., Wu, Y., Li, G., & Wang, F. (2007). Formation of hydrogen peroxide and degradation of phenol in synergistic system of pulsed corona discharge combined with TiO₂ photocatalysis. *Journal of Hazardous Materials*, *141*(1), 336–343. <https://doi.org/10.1016/j.jhazmat.2006.07.019>.
- Wang, T., Ma, T., Qu, G., Liang, D., & Hu, S. (2014). Performance evaluation of hybrid gas-liquid pulse discharge plasma-induced degradation of polyvinyl alcohol-containing wastewater. *Plasma Chemistry and Plasma Processing*, *34*(5), 1115–1127. <https://doi.org/10.1007/s11090-014-9565-x>.
- Wang, T., Qu, G., Sun, Q., Liang, D., & Hu, S. (2015a). Evaluation of the potential of p-nitrophenol degradation in dredged sediment by pulsed discharge plasma. *Water Research*, *84*, 18–24. <https://doi.org/10.1016/j.watres.2015.07.022>.
- Wang, T., Qu, G., Yan, Q., Sun, Q., Liang, D., & Hu, S. (2015b). Optimization of gas-liquid hybrid pulsed discharge plasma for p-nitrophenol contaminated dredged sediment remediation. *Journal of Electrostatics*, *77*, 166–173. <https://doi.org/10.1016/j.elstat.2015.08.011>.
- Wu, H., Fang, Z., & Xu, Y. (2015). Degradation of aniline wastewater using dielectric barrier discharges at atmospheric pressure. *Plasma Science and Technology*, *17*(3), 228–234. <https://doi.org/10.1088/1009-0630/17/3/10>.
- Xu, J. Q., Duan, W. H., Zhou, X. Z., & Zhou, J. Z. (2006). Extraction of phenol in wastewater with annular centrifugal contactors. *Journal of Hazardous Materials*, *131*(1–3), 98–102. <https://doi.org/10.1016/j.jhazmat.2005.09.011>.
- Xue, J., Chen, L., & Wang, H. (2008). Degradation mechanism of Alizarin Red in hybrid gas-liquid phase dielectric barrier discharge plasmas: experimental and theoretical examination. *Chemical Engineering Journal*, *138*(1–3), 120–127. <https://doi.org/10.1016/j.cej.2007.05.055>.
- Zhang, Q., Qu, G., Wang, T., Li, C., Qiang, H., Sun, Q., et al. (2017). Humic acid removal from micro-polluted source water in the presence of inorganic salts in a gas-phase surface discharge plasma system. *Separation and Purification Technology*, *187*, 334–342. <https://doi.org/10.1016/j.seppur.2017.06.053>.
- Zhu, L.-n., Ma, J., & Yang, S.-d. (2007). Removal of phenol by activated alumina bed in pulsed high-voltage electric field. *Journal of Environmental Sciences*, *19*(4), 409–415. [https://doi.org/10.1016/s1001-0742\(07\)60068-0](https://doi.org/10.1016/s1001-0742(07)60068-0).